



## 2. FEM Formulation for Analysis

The displacement and stress fields near the vertex in a three-dimensional stress state can be expressed in the asymptotic series in the case of real number of the order of stress singularity as follows:

$$\begin{aligned} \sigma_{ij} &\propto r^\lambda g_{ij}(\phi, \theta, \lambda) \\ u_i &\propto r^{\lambda+1} f_i(\phi, \theta, \lambda) \end{aligned} \quad (1)$$

where  $\lambda$  represents the order of stress singularity.  $r$  is the radial distance from the vertex,  $\phi$  and  $\theta$  are angles in the spherical coordinates as shown in Fig. 2. The angular variations of the displacement fields,  $f_i(\phi, \theta, \lambda)$ , and the stress fields,  $g_{ij}(\phi, \theta, \lambda)$ , are defined on a spherical domain of unit radius that surrounds the vertex ( $r \rightarrow 0$ ). When  $-1 < \lambda < 0$ , the stress singularity occurs. The distance  $r$  is expressed by using the singular transformation as

$$r = \rho r_o = r_o \left( \frac{1 + \alpha}{2} \right)^p \quad (2)$$

where  $p$  is an eigen value governing the stress field and  $p = \lambda + 1$ .  $r_o$  is a radius of the spherical domain and  $-1 < \alpha < 1$ . The displacement at the origin is set to zero, so the discretized displacement vector,  $u_i$ , at nodes can be expressed as

$$u_i = \rho^p \left[ \sum_{j=1}^8 H_j(\xi, \eta) u_{ij} \right] \quad (i = r, \theta, \phi) \quad (3)$$

where  $H_j(\xi, \eta)$  is the serendipity quadratic interpolation function.  $-1 \leq (\xi, \eta) \leq 1$ , and  $u_{ij}$  is the  $i$  component of displacement at node  $j$ . Angles  $\phi$  and  $\theta$  in the spherical coordinates are expressed using the interpolation function as follows:

$$\theta = \sum_{j=1}^8 H_j(\xi, \eta) \theta_j, \quad \phi = \sum_{j=1}^8 H_j(\xi, \eta) \phi_j \quad (4)$$

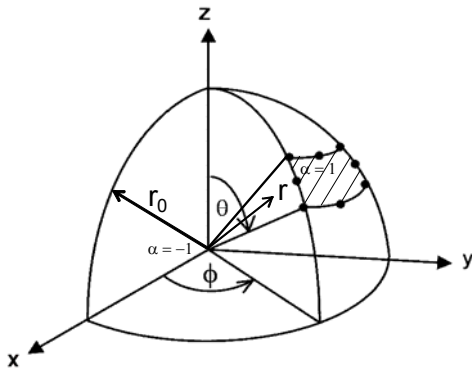


Figure 2 Finite element geometry and coordinate systems with the origin at the vertex of junction

Furthermore, strain is obtained by means of the chain rule differentiation as

$$\{\mathcal{E}\} = \begin{Bmatrix} \mathcal{E}_{rr} \\ \mathcal{E}_{\theta\theta} \\ \mathcal{E}_{\phi\phi} \\ \gamma_{r\theta} \\ \gamma_{r\phi} \\ \gamma_{\theta\phi} \end{Bmatrix} = \frac{\rho^{p-1}}{r_o} \sum_{i=1}^8 (p[B_{ai}] + [B_{bi}]) \{u_i\} = [B] \{u\} \quad (5)$$

where  $[B_{ai}]$  and  $[B_{bi}]$  are the 6x24 matrices. By using the principle of virtual work, the eigen value,  $p$ , can be calculated from the following characteristic equation.

$$(p^2[A] + p[B] + [C])\{U\} = 0 \quad (6)$$

where  $\{U\}$  is the eigen vector that represents the displacement fields at each node. This equation can be, then, transformed into the standard eigenvalue equation.

$$[S] \begin{Bmatrix} \bar{V} \\ \bar{U} \end{Bmatrix} = p \begin{Bmatrix} \bar{V} \\ \bar{U} \end{Bmatrix}, \quad [S] = \begin{bmatrix} 0 & I \\ -A^{-1}C & -A^{-1}B \end{bmatrix} \quad (7)$$

where  $\{\bar{V}\}$  is  $p\{\bar{U}\}$ .

## 3. Results and Discussion

In this section, the interface between solder bump and the other materials in FCOB package is shown in Fig. 3. At junction E, where solder bump, Cu pad, underfill and solder mark are bonded together, the relationship between  $\lambda$  and Young's modulus of solder bump,  $E_s$ , is investigated with varying the contact angle  $\omega$ . When the dimension governing the stress singularity is very small, the geometry of this junction seems to be the three-dimensional junction with a uniform cross section as shown in Fig. 4.

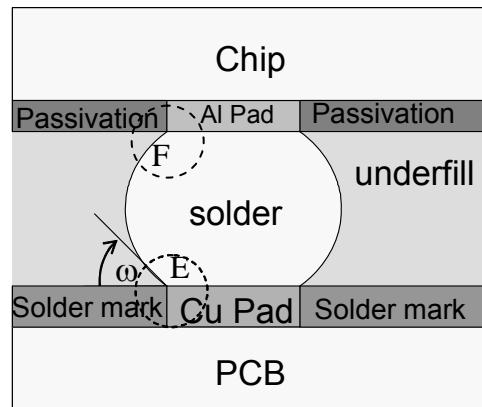


Figure 3 FCOB package configuration

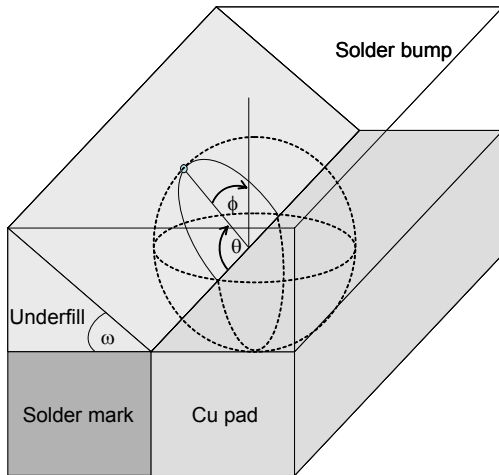


Figure 4 Junction E of FCOB package

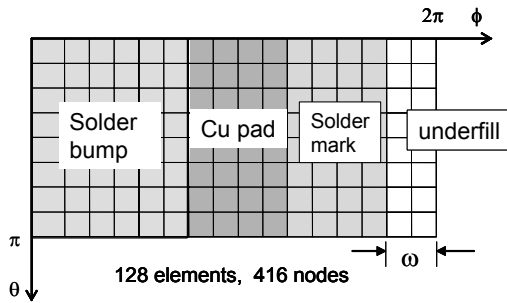


Figure 5 Mesh model of junction E of FCOB

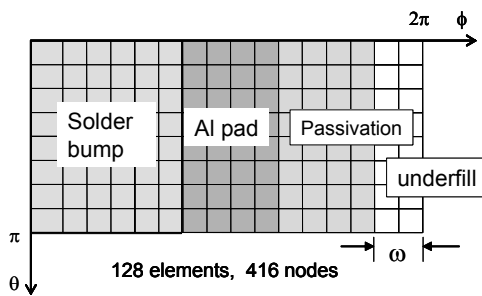


Figure 6 Mesh model of junction F of FCOB

The mechanical properties of material in the analysis are shown in Table 1. From the previous study (see Pageau *et al.* [10]), when a uniform mesh is applied the accuracy of the solution is satisfied. Therefore, in this paper, square mapped elements are used to create a mesh model. The number of integration points is 20x20 points and a model of fine mesh is used for yielding better results.

Table 1 Material properties in FCOB

Material	Elastic modulus (GPa)	Poisson's ratio
Cu pad	$E_{cu} = 76.0$	0.35
Al pad	$E_{al} = 70.0$	0.33
Solder mark	$E_{sm} = 8.0$	0.35
Solder bump	$E_s = 5.0$ to $40.0$	0.41
Underfill	$E_u = 6.0$	0.35
Passivation	$E_p = 310.0$	0.33

For the junction E (shown in Fig. 3), the variation of the order of stress singularity  $\lambda$  with varying  $E_s$  and the contact angle  $\omega$  is shown in Fig. 7. Poisson's ratio is fixed for all materials. For  $E_s$  is small (5 GPa to 7 GPa, almost identical to  $E_u$ ), it can be seen that  $\lambda$  changes a little as the contact angle  $\omega$  varies. However, when  $E_s$  is greater than 10 GPa, the absolute value of  $\lambda$  decreases obviously with increasing the contact angle  $\omega$ . It can be concluded that the reliability of the junction E can be improved as the proportion of underfill at the junction E increases. For example, the absolute value of  $\lambda$  is minimum at the angle  $\omega = 67.5^\circ$  for any value of  $E_s$ . Figure 8 shows the variation of  $\lambda$  with varying  $E_s$  and  $\omega$  at the junction F (in Fig. 3) which solder bump, passivation, Al pad and underfill are bonded to each other. The absolute value of  $\lambda$  increases obviously with increasing  $E_s$ . In the other hand, the absolute value of  $\lambda$  changes a little as the contact angle  $\omega$  varies. It means that the change of contact angle  $\omega$  at the junction F slightly influences on the order of stress singularity  $\lambda$ .

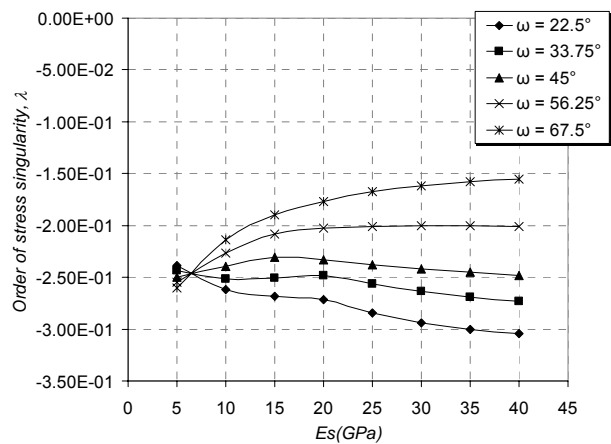


Figure 7 the variation of  $\lambda$  with varying  $E_s$  and  $\omega$  for the junction E of FCOB

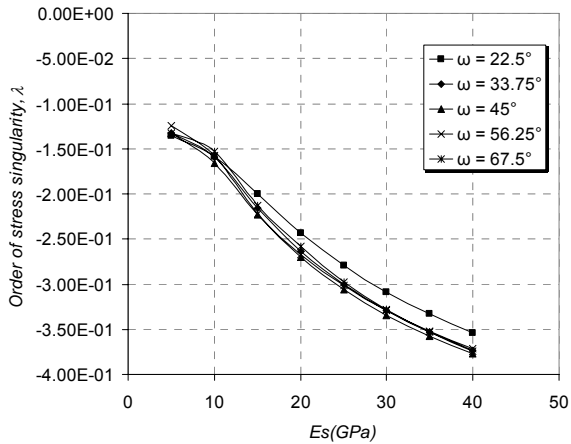


Figure 8 the variation of  $\lambda$  with varying  $E_s$  and  $\omega$  for the junction F of FCOB

The variation of  $\lambda$  with varying  $E_s$  and  $\omega$  at the junction F is different from that variation at the junction E, because Young's modulus of passivation  $E_p$  at the junction F is very large (310 GPa). Therefore, the change of proportion of underfill (varying the contact angle  $\omega$ ) at the junction F slightly affects the order of stress singularity  $\lambda$ .

#### 4. Conclusion

In the present paper, the order of stress singularity around the multi-material junctions of FCOB package was investigated using FEM eigen analysis. At the junction, the mechanical property of solder bump was varied while those of materials with high modulus, such as Cu, Al, and passivation were fixed. Furthermore, the contact angle at the junction also was varied. It can be concluded that the minimum order of stress singularity around the multi-materials junctions in FCOB package can be obtained with appropriate mechanical properties of solder bump and geometry of a junction.

#### 5. References

[1] Bogy, D. B., 1968. Edge-Bonded Dissimilar Orthogonal Elastic Wedges Under Normal and Shear Loading. *J. Appl. Mech.* 35, 460-466.

[2] Bogy, D. B., 1970. On the Problem of Edge-Bonded Elastic Quarter-Planes at the Boundary. *Int. J. Solids and Struct.* 6, 1287-1313.

[3] Bogy, D. B., 1971. Two-Edge Bonded Elastic Wedges of Different Materials and Wedge Angles Under Surface Traction-2. *J. Appl. Mech.* 38-2, 377-386.

[4] Bogy, D. B., 1971. On the plane Elastostatic Problem of a Loaded Crack Terminating at a Material Interface. *J. Appl. Mech.* 38, 911-918.

[5] Koguchi, H., 1997. Singularity Analysis in Three-Dimensional Bonded Structure. *Int. J. Solids Structures*, 34(4), 461-480.

[6] Koguchi, H., and Muramoto., 2000. The Order of Stress Singularity Near the Vertex in Three-Dimensional Joints. *Int. J. Solids Structures*, 37, 4737-4762.

[7] Koguchi, H., Yamashita, S., and Fujimagari, M., 2001. Three-Dimensional Stress Singularity Field Around a Vertex of Embedded Chip in Electronic Devices Using FEM. *Proceedings, ASME Interpack'01, USA.*

[8] Yamada, Y. and Okumura, H., 1981. Analysis of local stress in composite materials by the 3-D finite element. *Proc. of the Japan-U.S. Conference, Tokyo*, 55-64.

[9] Pageau, S. S., Joseph, P. F. and Biggers, S. B., 1994. The Order of Stress Singularities For Bonded and Disbonded Three-Material Junctions. *Int. J. Solids and Struct.* 31, 2979-2997.

[10] Pageau, S. S. and Biggers, S. B., Jr., 1995. Finite element Evaluation of Free-Edge Singular Stress Fields in Anisotropic Materials. *Int. J. Num. Method in Engineering*, 38, 2225-2239.

[11] Xu, A. Q. and Nied, H. F., 2000. Finite Element Analysis of Stress Singularities in Attached Flip Chip Packages. *ASME J. Electron. Packag.*, 122, 301-305.

[12] Liu, Y. H., Xu, J. Q., and Ding, H. J., 1999. Order of Singularity and Singular Stress Field about an Axisymmetric Interface Corner in Three-dimensional Isotropic Elasticity. *Int. J. Solids and Struct.*, 36, 4425-4445.